

**Forecasting  
wind-driven wildfires  
using an inverse  
modelling approach**

O. Rios et al.

This discussion paper is/has been under review for the journal Natural Hazards and Earth System Sciences (NHESS). Please refer to the corresponding final paper in NHESS if available.

# Forecasting wind-driven wildfires using an inverse modelling approach

O. Rios<sup>1</sup>, W. Jahn<sup>2</sup>, and G. Rein<sup>3</sup>

<sup>1</sup>CERTEC: Centre d'Estudis del Risc Tecnològic (Centre for Studies on Technological Risk)  
Department of Chemical Engineering, Universitat Politècnica de Catalunya, Av. Diagonal, 647,  
08028 Barcelona, Catalonia, Spain

<sup>2</sup>Raindance Science International, Santiago, Chile

<sup>3</sup>Department of Mechanical Engineering, Imperial College London, SW72AZ, London, UK

Received: 30 September 2013 – Accepted: 4 November 2013 – Published: 4 December 2013

Correspondence to: G. Rein (g.rein@imperial.ac.uk)

Published by Copernicus Publications on behalf of the European Geosciences Union.

Title Page

Abstract

Introduction

Conclusions

References

Tables

Figures



Back

Close

Full Screen / Esc

Printer-friendly Version

Interactive Discussion



fire breaks, back fires) and weather forecasts. More important, it must not require high computational resources (i.e. high performance computing or super computers) so that it can be developed flexibly in portable devices by fire responders.

## 1.1 Data assimilation and inverse modelling

Inverse modelling consists in studying the observed measurements from sensor data to gain information about the physical system behind them using a variety of mathematical models and techniques. Instead of just looking at the outputs of the model, inverse modelling knows the output and aims to unveil the parameters inside the physical system and the initial and boundary conditions of the problem.

The inverse method is particularly appropriate for wildfire modelling due to the large amount of unknowns in fires. The fuel properties and location, shape and the area covered by foliage, moisture content, meteorological conditions and topography are necessary variables to initialise a physical fire model but can hardly ever be measured. By contrast, the inverse approach can use any kind of available data if the forward model is tweaked accordingly.

Despite its promising capacity for coping with complex problems with a large number of variables, just few authors have tried to apply forecasting techniques to fire science. Among these, Jahn et al. (2011, 2012) successfully pioneered this approach to forecast fires in enclosures using both simple and complex models (two-zones model and computational fluid dynamics). In the field of wildfire, Mandel et al. (2009) explored this technique to predict the time-temperature curve of a sensor placed in the way of an advancing wildfire. They examined a reaction-diffusion equation and a semi-empirical fire line propagation model coupled with a Eulerian level-set-based equation. Additionally, they coupled weather forecast information to the model demonstrating the potential of data assimilation. Despite this progress, their implementation was found to be unstable due to the generation of spurious fires that cause non-physical results.

Rochoux et al. (2013) pioneered the application of real-time data assimilation to predict the location and spread of the wildfire front using infra-red sensors. Data were

## Forecasting wind-driven wildfires using an inverse modelling approach

O. Rios et al.

Title Page

Abstract

Introduction

Conclusions

References

Tables

Figures

⏪

⏩

◀

▶

Back

Close

Full Screen / Esc

Printer-friendly Version

Interactive Discussion



assimilated with a Kalman filter to balance computational and sensor errors. Rochoux et al.'s model assimilates perimeter locations at different times and uses the fuel depth as an input. The propagating model used two components: the rate of spread (RoS) represented by a product between the fuel depth ( $\delta$ ) and a constant ( $\Gamma$ ) to be quantified as part of the forecasting problem ( $\text{RoS} = \Gamma \cdot \delta$ ). Their model uses a level-set-based equation to cast the fire perimeter. Rochoux et al. tested the model in a controlled small scale experiment assimilating one fire front and delivering 30 s forecast.

## 1.2 Forecasting algorithm

We formulate the inverse problem based on the premise that some invariant exists by following the contributions of Jahn et al. (2012) on forecasting fire dynamics in enclosures. Invariants are the set of governing parameters that are mutually independent and constant for a significant amount of time. Therefore, our implementation relies on the assumption that some physical attributes of the system remain constant at least during some time. Those attributes can be uniform, a scalar or a vector field with spatial dependency. Examples of such quantity are initial fuel's moisture content or fuel depth. However, the invariants are not restricted to physical variables but can represent mathematical attributes of the system as well. For instance, if the wind speed changes but its effect on the RoS remains constant (boundary layer regime is maintained) the proper invariant will be its effect to the rate of spread rather than the wind speed itself.

After assimilating data during a period of time (assimilation windows) the invariants are estimated and used to forecast the perimeter evolution in the subsequent time interval. This forecast is then accurate until any of the invariants change significantly, which would be detected with the help of the continuous data feed from sensors. The sensor errors in the assimilated data are considered to be smaller than the model accuracy and therefore their influence is not directly considered here. This is a complementary approach to that of Rochoux et al. (2013) who balance data errors with model errors.

## Forecasting wind-driven wildfires using an inverse modelling approach

O. Rios et al.

Title Page

Abstract

Introduction

Conclusions

References

Tables

Figures



Back

Close

Full Screen / Esc

Printer-friendly Version

Interactive Discussion

Regarding sensor data feeds, in the present work we considered fire fronts positions hypothetically supplied by air-born observations, or ground crews. However, additional data such as flame height or spreading rate (recently measured by infra-red images and stereo vision Rossi et al., 2013) could be considered in future developments.

## 2 Building up the forward model

The initial step when posing an inverse modelling problem is to determine the forward model and its invariants. The forward model is the set of equations that relates the invariants to the observables. Its importance in the forecasting model is twofold: it is first used iteratively to quantify the invariants and then run again to deliver a forecast valid until the invariants change or the next assimilation process is started.

To create our forward model we combined Rothermel (1972) and Richards (1990) models. The Rothermel's model estimates the RoS of any point in the fire front whereas the Richard's model uses these RoS to generate the elliptical wavelets – firelets – that expand the fire front and computes its location at any time.

### 2.1 Rothermel's model

Rothermel's model is based on an energy balance equation where the heat sources and sinks are identified to estimate the RoS of a surface fire. The original formulation uses several experimental correlations deduced from data obtained in wind-tunnel experiments using fuel beds of varying conditions. The model was derived for fires that are in a quasi-steady spread state. This means that any acceleration of the fire is not considered. The shape of the fire front is assumed to have no influence on the RoS.

Rothermel's equation can be recast with three invariants ( $I_x$ ), defined as follows:

$$\text{RoS} = I_{mf}(1 + I_u \cdot I_w) \quad (1)$$

$I_{mf}$  captures the effect of all the fuel properties; oven-dry fuel loading ( $w_o$ ), surface-area-to-volume ratio ( $\sigma$ ), moisture content ( $M_f$ ), moisture of extinction ( $M_x$ ) and fuel depth

## Forecasting wind-driven wildfires using an inverse modelling approach

O. Rios et al.

Title Page

Abstract

Introduction

Conclusions

References

Tables

Figures



Back

Close

Full Screen / Esc

Printer-friendly Version

Interactive Discussion



( $\delta$ ).

$$I_{mf} = \mathcal{F}(\sigma, w_o, \delta, M_f, M_x) \quad (2)$$

The wind speed is directly equal to  $I_u$ :

$$I_u = U \quad (3)$$

5 The effect of the wind speed on the fire spread also depends on fuel properties such as layout, bulk density, surface-area to volume ratio and fuel depth. Its effect is embedded in  $I_w$  as:

$$I_w = \mathcal{K}(\sigma, w_o, \delta) \cdot U^{B-1} \quad (4)$$

Where  $B$  is an empirical coefficient determined by Rothermel (1972).

## 10 2.2 Huygens principle

Although Rothermel's model can estimate the RoS of any point, it is a mean value for the head fire only (Rothermel, 1972) and does not inform about different directions of spread. Therefore, it is not sufficient in predicting the fire front shape and location. In parallel to RoS estimation, some other model must be used to represent the fire perimeter expansion. We used Huygens principle – originally postulated to explain light wavefront propagation – with elliptical expansion, as proposed by Richards (1993). Applying it to wildfire, this principle considers every point in the fire perimeter at time  $t$  as a new ignition source that spreads during a time  $dt$  following an elliptical template shape – known as *firelet*. The corresponding fire front line at time  $t + dt$  is the outer curve that envelopes the firelets centred on the rear focus as showed in Fig. 1.

20 The details of the Huygens firelet model can be found in Richards (1990, 1993), but an overview of the main concepts and equations is provided here.

Considering the initial ignition point situated at  $\{X_0, Y_0\}$  and using a parameterisation variable  $s \in [0 - 2\pi]$ , the  $\{(x_i(t), y_i(t))\}$  coordinates of fire front vertexes can be analytically calculated by integrating a set of partial differential equations:

$$x(s, \hat{t}) = X_0 + \int_0^{\hat{t}} \left( \frac{a^2(t) \cos \theta(t) \cos(K) + b^2(t) \sin \theta(t) \sin(K)}{\sqrt{a^2(t) \cos^2(K) + b^2(t) \sin^2(K)}} \cdot c(t) \sin \theta(t) \right) dt \quad (5)$$

$$y(s, \hat{t}) = Y_0 + \int_0^{\hat{t}} \left( \frac{a^2(t) \sin \theta(t) \cos(K) + b^2(t) \cos \theta(t) \sin(K)}{\sqrt{a^2(t) \cos^2(K) + b^2(t) \sin^2(K)}} \cdot c(t) \cos \theta(t) \right) dt \quad (6)$$

Where,

$$K = \theta(t) + s \quad (7)$$

Where  $\theta$  is the wind direction and  $b$  and  $c$  are lateral and backwards propagation velocities that can vary spatially and are calculated by imposing Rothermel's rate of spread for the head fire from the new ignition point:

$$b(s, t) + c(s, t) \equiv \text{RoS}(s, t) \quad (8)$$

The lateral front velocity  $a$ , however, is directly related to the eccentricity of the firelet. It was originally estimated using an experimental correlation found by Anderson (1983) that relates the ratio between the major and the minor firelet's axis, and thus, the ratio between  $b$  and  $a$  (independent of the time step  $\Delta t$  used). Its value depends on the wind speed ( $U$ ) in accordance with the equation:

$$\frac{a}{b} = 0.936e^{0.2566U} + 0.461e^{-0.1548U} - 0.397 \equiv \text{LB} \quad (9)$$

Note that the power coefficients in this empirical equation have units of  $[\text{s m}^{-1}]$  and LB is called length-to-breadth ratio and accounts for the eccentricity of the elliptical firelets.

**Forecasting  
wind-driven wildfires  
using an inverse  
modelling approach**

O. Rios et al.

Title Page

Abstract

Introduction

Conclusions

References

Tables

Figures

⏪

⏩

◀

▶

Back

Close

Full Screen / Esc

Printer-friendly Version

Interactive Discussion



The constant 0.397 is a modification of Anderson's original formula to ensure that the fire expands circularly ( $LB = 1$ ) under no-wind conditions ( $U = 0$ ).

Once the length-to-breadth ratio is known,  $a$ ,  $b$ ,  $c$  velocities can be calculated using Eq. (8) and the elliptical geometry properties:

$$a = \text{RoS} \frac{1 + 1/\text{HB}}{2\text{LB}} \quad (10)$$

$$b = \text{RoS} \frac{1 + 1/\text{HB}}{2} \quad (11)$$

$$c = b - \frac{\text{RoS}}{\text{HB}} \quad (12)$$

where,

$$\text{HB} = \frac{\text{LB} + \sqrt{\text{LB}^2 - 1}}{\text{LB} - \sqrt{\text{LB}^2 - 1}} \quad (13)$$

If the invariant  $I_u = U$ , introduced in Rothermel's model, is reused in Huygens' firelets expansion, only one additional invariant is required to account for the principal direction of spreading determined by the wind direction:

$$I_\theta = \theta \quad (13)$$

The forward model is then a function of four invariants:

$$\mathcal{M}(I_u, I_w, I_{mf}, I_\theta, T) = \begin{cases} \text{RoS} = \mathcal{R}_t(I_u, I_w, I_{mf}) \\ \{x, y\} = \mathcal{H}(\text{RoS}, I_u, I_\theta, T) \end{cases} \quad (14)$$

Where  $T$  is the time when the fire front is estimated,  $\mathcal{R}$  represents Rothermel's model with cast invariants (Eq. 1) and  $\mathcal{H}_t$  the firelet expansion (from Eq. 5 to 6).

**Forecasting wind-driven wildfires using an inverse modelling approach**

O. Rios et al.

Title Page

Abstract

Introduction

Conclusions

References

Tables

Figures

⏪

⏩

◀

▶

Back

Close

Full Screen / Esc

Printer-friendly Version

Interactive Discussion



Discussion Paper | Discussion Paper | Discussion Paper | Discussion Paper | Discussion Paper

Depending on the acquirable sensor data, the invariants can be turned into input data for the problem. For example, if reliable wind speed data arrive, there is no need to solve for it but instead it is directly used as input in the forward model. The assimilating data algorithm actually imbibes both, measured and forecasted data, to deliver the most accurate forecast.

### 2.3 Cost function

The invariants are calculated by minimizing a cost function  $J$  that measures the difference between the model output and the sensor observations. The cost function proposed is the Euclidean norm summed over the different assimilation times.

$$J(\boldsymbol{\rho}) = \sum_{t=t_i}^{t_f} \sqrt{[\mathbf{x}_i - \hat{\mathbf{x}}_i(\boldsymbol{\rho})]^T \mathbf{W}_i [\mathbf{x}_i - \hat{\mathbf{x}}_i(\boldsymbol{\rho})]} \quad (15)$$

Where  $\{\mathbf{x}_i\} \in \mathbb{R}^2$  are the  $N$ -coordinates set of the observed fire front position in a given time step  $i$  and  $\hat{\mathbf{x}}_i(\boldsymbol{\rho}) = \mathcal{M}_x(\boldsymbol{\rho})$  are the corresponding model output position for a set of invariants  $(\boldsymbol{\rho})$ .  $\mathbf{W}_i$  is a weigh function that could be used to give more value to the latest assimilation on time in order to better capture the invariants to create the forecasting. However, in the present work no weighting function is used ( $\mathbf{W}_i = \mathbb{I}$ ) but the framework is set to allow introductions of non-uniform weights to the sensors in future work (for example to give more importance to IR images than to in-situ visual observations).

Equation (15) can be simplified if the  $\mathbf{x} - \mathbf{y}$  coordinates (both, observables and model output) are concatenated as 1-row vector  $\tilde{\mathbf{y}}_i$  and  $\tilde{\mathbf{y}}_i = \mathcal{M}_i(\boldsymbol{\rho})$ :

$$J(\boldsymbol{\rho}) = \sum_{t=t_i}^{t_f} \sqrt{[\tilde{\mathbf{y}}_i - \tilde{\mathbf{y}}_i(\boldsymbol{\rho})]^T [\tilde{\mathbf{y}}_i - \tilde{\mathbf{y}}_i(\boldsymbol{\rho})]} \quad (16)$$

Although the square root gives the correct Euclidean norm, it does not effect the minimisation and therefore we removed it from the computational implementation.

## Forecasting wind-driven wildfires using an inverse modelling approach

O. Rios et al.

Title Page

Abstract

Introduction

Conclusions

References

Tables

Figures

⏪

⏩

◀

▶

Back

Close

Full Screen / Esc

Printer-friendly Version

Interactive Discussion



## 2.4 Optimisation

There are two main approaches to minimize Eq. (16); the gradient-free and the gradient-based (Nocedal and Wright, 1999). The first group are stochastic algorithms that evaluate the cost function  $\mathcal{J}(\boldsymbol{p})$  at many random points to find the absolute minimum, whereas the second group use an initial guess (called background vector,  $\boldsymbol{p}^b$ ) and follow the gradient direction towards the closest minimum. Although gradient-free algorithms can sweep a broader search space to find the absolute minimum, they have to evaluate the cost function multiple times which might be computationally costly if the forward model  $\mathcal{M}(\boldsymbol{p})$  is complex. On the other hand, when the cost function is continuous and the possible domain of the invariants ( $\boldsymbol{p}$ ) is known and delimited (as it is in our problem), the gradient-based algorithms are more suitable and efficient. It is true that gradient-based algorithms can converge to a local minima instead of a global one. However, the extended sensitivity analysis performed on our problem showed that the system is benign in the sense that all the functions involved behave smoothly and therefore the convergence to the absolute minima will depend on the initial guess.

If the forward model  $\mathcal{J}(\boldsymbol{p})$  is linear then the cost function is quadratic and can be minimised by easily solving a system of linear equations (as will be shown in the following sections). For forward models that are not linear – as it is the case – the Tangent Linear Model (TLM) has been widely used to tackle the problem (Griewank, 2000).

## 2.5 Tangent Linear Model

TLM consist in linearising the forward model  $\mathcal{M}(\boldsymbol{p})$  in the vicinity of an initial guess  $\boldsymbol{p}^b$ . This linearisation can be done if the model is weakly non linear as the one at hand. The viability of the TLM relies on the initial guess and the fact that the procedure is iterated until convergence. To calculate the TLM we use first order Taylor's series expansion around  $\boldsymbol{p}^b$ :

## Forecasting wind-driven wildfires using an inverse modelling approach

O. Rios et al.

Title Page

Abstract

Introduction

Conclusions

References

Tables

Figures

⏪

⏩

◀

▶

Back

Close

Full Screen / Esc

Printer-friendly Version

Interactive Discussion

## Forecasting wind-driven wildfires using an inverse modelling approach

O. Rios et al.

Title Page

Abstract

Introduction

Conclusions

References

Tables

Figures

◀

▶

◀

▶

Back

Close

Full Screen / Esc

Printer-friendly Version

Interactive Discussion



The gradient of the linearized function is then:

$$\nabla_{\rho} \mathcal{J}(\rho) = 2 \sum_{t=t_i}^{t_f} \left[ \left( \nabla_{\rho} \mathcal{M}_i(\rho^b)(\rho - \rho^b) \right) \right]^T \left[ \bar{y}_i - \left( \mathcal{M}_i(\rho^b) + \nabla_{\rho} \mathcal{M}_i(\rho^b)(\rho - \rho^b) \right) \right] \quad (17)$$

Applying the first order condition for minimisation and introducing the following notation:

$$\mathbf{M}_i = \mathcal{M}_i(\rho^b)$$

$$\mathbf{H}_i = \nabla_{\rho} \mathcal{M}_i(\rho^b)$$

$$\bar{\rho}_i = (\rho - \rho^b)$$

Becomes:

$$\sum_{t=t_i}^{t_f} \mathbf{H}_i^T \mathbf{H}_i \bar{\rho} = \sum_{t=t_i}^{t_f} \mathbf{H}_i^T (\bar{y}_i - \mathbf{M}_i) \quad (18)$$

which is a linear system that can be easily solved by using a QR factorisation with column pivoting (Nocedal and Wright, 1999).

## 2.6 Automatic differentiation

Calculating the jacobian multiplication term  $\mathbf{H}_i^T \mathbf{H}_i$  in Eq. (18) requires partially differentiating the model with respect to the different invariants. This has to be done  $p \times 2n \times t$  times, where  $p$  is the number of invariants used,  $2n$  the coordinates of the fire front and  $t$  the assimilating time.

The simplest way to numerically evaluate the jacobian is by finite centred differences:

$$\mathbf{H}_{k,i}^j = \frac{\partial \mathcal{M}_i^j(\rho^b)}{\partial \rho_k} \simeq \frac{\mathcal{M}_i^j(\rho^b + \epsilon_k) - \mathcal{M}_i^j(\rho^b)}{\|\epsilon_k\|}$$





## 2.8 Synthetic data

In order to better to investigate in detail all the capabilities of the forecasting model, it is validated with synthetic data that works as an controlled-experiment before challenging it with real complex data. The synthetic data were generated also by a Rothermel–Huygens firelet expansion model with all the correlated formulas and experimental values embedded. Fuels properties provided by Scott and Burgan (2005) were used to initialise the model. The synthetic data are input to the forecasting algorithm in due time trying to mimic the data acquisition in a real situation.

## 3 Results

The forecasting algorithm developed in this article is investigated in different situations where synthetic data simulates the observations to assimilate. The tests are performed varying different parameters like the assimilation window, assimilated data (fire fronts locations and feeding frequency) and initial guess. Then we look at several features like convergence of the invariant, minimisation of the cost function, effect of the initial guess, effect of the assimilating window width, the computing time and the leading times obtained.

However, the same methodology is applied and explored with alternative invariants to handle more realistic situations where some of the physical quantities assumed as constant are allowed to vary.

In all of the following tests, punctual ignition source is considered as the initial integration point for the fire front expansion. This ignition point source is depicted as a red spot in all the perimeter-expansion plots and is a required piece of information to run the forecasting algorithm. In a real wildfire situation, it could be identified as the first reported location of the fire – the bottom of the smoke plume, as an example. If the fire has spread out before the first bit of information arrives and it is no longer a point

## Forecasting wind-driven wildfires using an inverse modelling approach

O. Rios et al.

Title Page

Abstract

Introduction

Conclusions

References

Tables

Figures



Back

Close

Full Screen / Esc

Printer-friendly Version

Interactive Discussion

source, the first assimilated fire front can be also used as a virtual ignition perimeter by considering the whole fire front as a set of initial ignition sources.

### 3.1 Initial guess

Apart from the assimilated data, the forecasting algorithm needs an initial guess of the invariant value where the first Tangent Linear Approximation (TLM) is performed. This first educated guess can be directly generated within the range of validity of each invariant – without considering any hint from the actual wildfire – or by using Rothermel equivalent equations (Eqs. 2–4 and 13) and guesstimating the six physical underlying quantities  $\delta$ ,  $M_f$ ,  $M_x$ ,  $\sigma$ ,  $W_0$  and  $\theta$  which can be roughly done by observing the fuel and wind.

To perform a rigorous study of the effect of the initial guess, the six initialising variables were swept according to operational-based considerations. For instance, the fuel depth  $\delta$  was considered to be an easily estimable variable in a real wildfire (it can be easily distinguished between 5 cm pine needle litter or 1 m tall grass) and thus, its offset in the initial guess is considered to be lower than 1.50 m. In contrast, some other variables such as moisture content ( $M_{mf}$ ) or oven-dry fuel loading ( $w_0$ ), cannot be estimated with such accuracy and therefore the educated guess exploration covers a larger differing range.

### 3.2 Quantifying the invariants

The first scenario investigated here assimilates 15 fire fronts with a window width of 15 min. (i.e. one fire front per min.). The invariants converge within 3 iterations (i.e. 3 runs of TLM and thus, 3 estimations of the invariants). Figure 3 shows the observed data (black triangles), the fronts generated with the initial invariants guess (red dashed lines) and the respective fire fronts after each iteration (dashed lines) until convergence is reached (green solid line). The invariants and cost function convergence are depicted in Fig. 4. The cost function (dashed line) shows a rapid decrease towards zero. Its slope

## Forecasting wind-driven wildfires using an inverse modelling approach

O. Rios et al.

Title Page

Abstract

Introduction

Conclusions

References

Tables

Figures



Back

Close

Full Screen / Esc

Printer-friendly Version

Interactive Discussion



quantifies the converging rate. At the first iteration the slope is steep which indicates that the algorithm quickly corrects the large discrepancies. As the cost decreases so does the steepness indicating that convergence is achieved since in a minimum the steepness flattens.

5 In the case shown in Fig. 4 (bottom) all invariants converge to true value within 2% of percentage difference.

### 3.3 Assimilation window width

The window width (WW) is the amount of time while the forecasting algorithm is being fed data (i.e. fire front location in the case at hand). The time between consecutive fire front observations is called assimilation period ( $T$ ) and can be directly related to the assimilating frequency ( $F = 1/T$ ).

15 The main effect of the number of assimilated fronts ( $WW/T$ ) is the resolution of multiplicity. The value of the cost function tends to increase as the assimilation window increases and more fronts are assimilated. The error of the initial guess amplifies with the propagation (the previous fire front position is required to calculate the new one) and therefore the forecasting algorithm is more sensitive to the wrong identification of invariants. This is shown in Fig. 5 where instead of assimilating 15 min (and 15 fire fronts) – as in the converging example above – we assimilate front positions during 3 min (i.e. 3 front positions). The cost function rapidly drops to zero but in this case the value estimated for both  $I_{mf}$  and  $I_w$  differs from the true value by 10%. The reason is that now the initial cost function has a lower absolute value since the propagation of an inaccurate estimation is truncated in time and therefore the effects of an incorrect assimilation are hidden. It is worth mentioning that despite the possibility of  $I_{mf}$  and  $I_w$  misconverging, RoS is always correctly estimated as it has no multiplicity in the forward model and only one value can fit the observations.

25 One way to deal with multiplicity is by defining only one invariant for the RoS. This approach, however, does not allow for the forecasting algorithm to be ameliorated if any extra data are available (as will be done in Sect. 3.4) since no information about par-

## Forecasting wind-driven wildfires using an inverse modelling approach

O. Rios et al.

Title Page

Abstract

Introduction

Conclusions

References

Tables

Figures



Back

Close

Full Screen / Esc

Printer-friendly Version

Interactive Discussion



## Forecasting wind-driven wildfires using an inverse modelling approach

O. Rios et al.

Title Page

Abstract

Introduction

Conclusions

References

Tables

Figures



Back

Close

Full Screen / Esc

Printer-friendly Version

Interactive Discussion



5 ticular contributions is achieved. Thus, a more interesting way to diminish multiplicity is to recast the invariants and input extra data in a way that the invariants become functionally independent. For instance, if the fuel-moisture invariant is somehow multiplied by any measurable quantity (as fuel depth or moisture content) that varies spatially or over time, then, its value is no longer exchangeable with the wind factor. The same strategy could be used for this second invariant if wind speed is known. This approach is successfully explored in the following sections.

10 The third way to deal with multiplicity is by assimilating additional quantities that are predicted by the forward model. It is worth pointing out the difference between inputting additional values and assimilating more information. The first consists of extra inputs to run the forward model and allows it to handle more complex situation. Examples of this could be information of moisture content, fuel properties or wind speed. Data assimilation, in contrast, requires the quantifiable information to be the output of the forward model. Thus, in our case, only the positions of the fronts can be assimilated but  
 15 the forward model can be complemented so it delivers additional characteristics such as flame height or fire intensity. By assimilating this additional information the invariant multiplicity is narrowed down since each invariant is then part of different equations and they are no longer dependent.

### 3.4 Forecasting the fire spread

20 Once the invariants are identified, the forecasting algorithm predicts the location of the fire by running the forward model again with the correct invariants. The forecast will be valid as long as the conditions present when assimilating the data remain constant.

In order for it to be an operative tool, the forecasting algorithm must deliver the forecast ahead of the event, thus, any forecast must meet the positive lead time requirement. The lead time is defined as the amount of time between the delivery of the  
 25 forecast and the predicted event. If the forecasting algorithm needs 1 min (computing time) to deliver a 20 min forecast then the lead time is 19 min.

## Forecasting wind-driven wildfires using an inverse modelling approach

O. Rios et al.

Title Page

Abstract

Introduction

Conclusions

References

Tables

Figures

⏪

⏩

◀

▶

Back

Close

Full Screen / Esc

Printer-friendly Version

Interactive Discussion



The lead time principally depends on the number of assimilated fronts and the initial guess (i.e. iterations required for convergence). The forecasting time (either we ask for a 15 min or 45 min forecast) also plays a role when the forward model is computationally demanding. However, due to the simplicity of the forward model used in the case at hand, its contribution is limited as shown in Fig. 6.

### 3.5 Different data contexts

The invariants can be adapted to different data situations. To show the versatility of our model two different cases with different available data are presented as example.

In the first case wind speed and direction are provided and assumed to be spatially independent – same wind speed and direction for all the fire perimeter – although can vary on time. By contrast, in the second case, the fuel depth  $\delta$  is allowed to vary spatially, which increases the validity of the model for heterogeneous situations. Both cases rely on realistic measuring capabilities in a real fire. Wind speed and direction can be gathered from deployed units as well as from weather stations spread over the fire area. Regarding the information about fuel, forest managers usually map forest areas in advance to list their spatially distributed characteristics. New techniques recently brought into the field such as the use of LIDAR – Light Detection and Ranging (Mutlu et al., 2008), potentially increases the accuracy and availability of this information and opens the door for preparing operative measuring systems for the situations when these data are not known.

#### 3.5.1 Wind speed as sensor data

The first step is to recast the invariants related to wind speed and wind direction which can be directly done by reversing  $I_u$  and  $I_\theta$  into input variables. Then  $I_w$  is redefined using the wind factor functional relation from Rothermel:

$$\Phi_w = CU^B \left( \frac{\beta}{\beta_0} \right)^{-E} = \mathcal{P}(\sigma, \beta, w_0, \delta) \cdot U^B = I_{w_1} \cdot U^{I_{w_2}} \quad (19)$$

Thus,

$$I_{w_1} = \mathcal{P}(\sigma, w_0, \delta) = C \left( \frac{\beta}{\beta_0} \right)^{-E} \quad (20)$$

$$I_{w_2} = \mathcal{F}(\sigma) = B \quad (21)$$

5 Where  $C$  and  $B$  are calculated with experimental correlations derived by Rothermel and  $\beta, \beta_0$  are the nominal and the optimal packing ratio respectively.

The other invariant  $I_{mf}$  remain the same and, thus, the model is described by three invariants plus the simulation time  $T$ .

$$\mathcal{M}(I_{w_1}, I_{w_2}, I_{mf}, T) = \begin{cases} \text{RoS} = \mathcal{R}_t(I_{w_1}, I_{w_2}, I_{mf}) \\ \{x, y\} = \mathcal{H}(\text{RoS}, I_u, I_\theta, T) \end{cases} \quad (22)$$

10 The reason why three degrees of freedom are needed despite the new assimilated data is because the effect of the wind in the RoS and the firelets shape is still unknown as it depends on several fuel parameters as such the packing ratio or oven-dry bulk density. However, the important difference is that now the wind is allowed to change (is not an invariant any more) and, therefore, the forecasting algorithm can deal with more complicated – less idealised – situations.

15 Despite this recast being, to some extent, more complicated than the previous one, it allows to identify the invariants more accurately than the previous recast. Nevertheless, on average, more iterations are needed to reach the required convergence which slightly increases the computing time. Figure 7 shows the perfect convergence of the invariants to true value with this recast.

25 Besides considering observed values for wind speed and direction, the forecast algorithm can also consider meteorological predictions to deliver a more accurate forecast when these quantities vary. To illustrate this, five fire fronts are assimilated during 25 min (at a frequency of 1 fire front every 5 min). The invariants are perfectly identified with six iterations as shown in Fig. 7. Then, a forecast is launched for the next 25 min with a synthetic prediction of wind speed and direction.

---

**Forecasting  
wind-driven wildfires  
using an inverse  
modelling approach**

O. Rios et al.

---

Title Page

Abstract

Introduction

Conclusions

References

Tables

Figures

⏪

⏩

◀

▶

Back

Close

Full Screen / Esc

Printer-friendly Version

Interactive Discussion





**Forecasting wind-driven wildfires using an inverse modelling approach**

O. Rios et al.

|                          |              |
|--------------------------|--------------|
| Title Page               |              |
| Abstract                 | Introduction |
| Conclusions              | References   |
| Tables                   | Figures      |
| ⏪                        | ⏩            |
| ◀                        | ▶            |
| Back                     | Close        |
| Full Screen / Esc        |              |
| Printer-friendly Version |              |
| Interactive Discussion   |              |

its contribution is linear in our forward model but might be important if more complex forward models are to be used (such as CFD based, for example). The Rothermel's variables that generate the synthetic data and the educated guess were kept constant for all the scenarios when they were not an input parameter (as wind speed, wind direction or fuel depth).

Figure 10 depicts the computing time vs. the number of assimilated fronts. The invariant cast for the situation when wind speed and direction are known parameters (red solid line) turns out to be the faster case. As expected, decreasing the number of invariants to be identified, speeds up the model since the dimension of the matrices involved in the optimisation process decreases. The exception is when fuel information is input (light blue lines). The spatial dependency of the fuel depth and the fact that RoS has to be recalculated in every node raises the computing time and thus, this case is the slower one. The effect of feeding the algorithm with wind speed becomes noticeable above 16 assimilated fronts when the complexity of the fire fronts shapes increases the number of iterations required to reach convergence.

Despite these significant differences, when eight fronts are assimilated the forecast is delivered in less than one min and even when 24 fronts are assimilated the lead time is well above 25 min for a 30 min forecast.

A laptop with dual processor core of 2.2 GHz is used as a computational tool since (as stated in the initial requirements) the forecasting algorithm must be suitable for desktop computers.

**3.7 Effect of errors in the data**

The fact that the synthetic data is generated with a Rothermel's–Huygens model implies that it exists at least one true invariant vector that exactly generates the observed fronts. However, this is not the case in reality since the forward model used is only an approximation of the real fire dynamics. Thus, to test the forecasting algorithm in a situation where such a true vector does not exist any more (thus, perfect convergence is then impossible), the synthetic data used in the fuel depth input data case





## Forecasting wind-driven wildfires using an inverse modelling approach

O. Rios et al.

Title Page

Abstract

Introduction

Conclusions

References

Tables

Figures



Back

Close

Full Screen / Esc

Printer-friendly Version

Interactive Discussion



special attention must be taken regarding multiplicity in the determination of the invariants. Multiplicity can be avoided by extending the forward model so it predicts extra parameters (as flame height or heat release rate) and assimilate them, or including extra information about the system to break the multiplicity. The later was implemented and illustrated in 2 different scenarios. All the invariants were then correctly identified, even when the first guess greatly differed from the true value. All the implementations had a positive lead time (time ahead of the event). The most computing expensive implementation is the one that uses fuel depth since the RoS varies in each node of the front.

After all the evaluations performed to the different implementation of the operational forecasting algorithm, we can conclude that we set up the framework for a promising forecasting tool and proposed first simple yet powerful implementations.

The next required step to make this algorithm operational is to check it with real data. To keep developing the methodology some identified limitations should be tackled as spotting fires – which does not follow classical (i.e. Rothermel's) fire spread – and the capacity of the forecasting algorithm to deal with uncertainties caused by the lack of reliable data, and deliver probabilistic values as outputs. To pursue this, we propose to explore more sophisticated forward models (pyrolysis, CFD) and greatly increase the number of invariants to several dozen. Then the automatic direct differentiation should be switched to adjoint differentiation (adjoint modelling approach) to keep the low computational cost requirement.

*Acknowledgements.* The support for O. Rios from the Erasmus Mundus European Project and the International Master of Science in Fire Safety Engineering (IMFSE) is gratefully acknowledged. The authors also want to thank Elsa Pastor for comments that improved draft versions.

## References

- Anderson, H. E.: Predicting wind-driven wild land fire size and shape, US Department of Agriculture, Forest Service, Intermountain Forest and Range Experiment Station, 1983. 6929
- Cowlard, A., Jahn, W., Abecassis-Empis, C., Rein, G., and Torero, J. L.: Sensor assisted fire fighting, *Fire Technol.*, 46, 719–741, 2010. 6924
- 5 Finney, M.: FARSITE, fire area simulator – model development and evaluation, vol. 3, US Department of Agriculture, Forest Service, Rocky Mountain Research Station, 1998. 6948
- Griewank, A.: Evaluating Derivatives: Principles and Techniques of Algorithmic Differentiation, no. 19 in *Frontiers in Appl. Math.*, SIAM, Philadelphia, PA, 2000. 6932, 6934
- 10 Jahn, W., Rein, G., and Torero, J. L.: Forecasting fire growth using an inverse zone modelling approach, *Fire Safety J.*, 46, 81–88, 2011. 6924, 6925
- Jahn, W., Rein, G., and Torero, J. L.: Forecasting fire dynamics using inverse computational fluid dynamics and tangent linearisation, *Adv. Eng. Softw.*, 47, 114–126, 2012. 6925, 6926
- Mandel, J., Bennethum, L. S., Beezley, J. D., Coen, J. L., Douglas, C. C., Kim, M., and Voldacek, A.: A wildland fire model with data assimilation, *Math. Comput. Simulat.*, 79, 584–606, 15 2008. 6924
- Mandel, J., Beezley, J. D., Coen, J. L., and Kim, M.: Data assimilation for wildland fires, *IEEE Contr. Syst. Mag.*, 29, 47–65, 2009. 6925
- Mutlu, M., Popescu, S. C., Stripling, C., and Spencer, T.: Mapping surface fuel models using lidar and multispectral data fusion for fire behavior, *Remote Sens. Environ.*, 112, 274–285, 20 2008. 6940
- Nocedal, J. and Wright, S. J.: *Numerical Optimization*, Springer Series in Operations Research and Financial Engineering, Springer, New York, 1999. 6932, 6933
- Richards, G. D.: An elliptical growth model of forest fire fronts and its numerical solution, *Int. J. Numer. Meth. Eng.*, 30, 1163–1179, 1990. 6927, 6928
- 25 Richards, G. D.: The properties of elliptical wildfire growth for time dependent fuel and meteorological conditions, *Combust. Sci. Technol.*, 95, 357–383, 1993. 6928
- Rochoux, M. C., Delmotte, B., Cuenot, B., Ricci, S., and Trouvé, A.: Regional-scale simulations of wildland fire spread informed by real-time flame front observations, *P. Combust. Inst.*, 34, 2641–2647, 2013. 6924, 6925, 6926
- 30 Rossi, J., Molinier, T., Akhloufi, M., Pieri, A., and Tison, Y.: Advanced stereovision system for fire spreading study, *Fire Safety J.*, 60, 64–72, 2013. 6927

## Forecasting wind-driven wildfires using an inverse modelling approach

O. Rios et al.

Title Page

Abstract

Introduction

Conclusions

References

Tables

Figures



Back

Close

Full Screen / Esc

Printer-friendly Version

Interactive Discussion



Rothermel, R.: A mathematical model for predicting fire spread in wildland fuels, Intermountain Forest & Range Experiment Station, Forest Service, US Department of Agriculture, 1972. 6927, 6928

5 Scott, J. and Burgan, R.: Standard fire behavior fuel models : a comprehensive set for use with Rothermel's surface fire spread model, USDA Forest Service, Rocky Mountain Research Station, General Technical Report RMRS-GTR-153, 72 pp., 2005. 6936

Sullivan, A. L.: Wildland surface fire spread modelling, 1990–2007. 3: Simulation and mathematical analogue models, Int. J. Wildland Fire, 18, 387–403, 2009. 6924

# NHESSD

1, 6923–6959, 2013

## Forecasting wind-driven wildfires using an inverse modelling approach

O. Rios et al.

Title Page

Abstract

Introduction

Conclusions

References

Tables

Figures



Back

Close

Full Screen / Esc

Printer-friendly Version

Interactive Discussion



## Forecasting wind-driven wildfires using an inverse modelling approach

O. Rios et al.

Title Page

Abstract

Introduction

Conclusions

References

Tables

Figures

◀

▶

◀

▶

Back

Close

Full Screen / Esc

Printer-friendly Version

Interactive Discussion

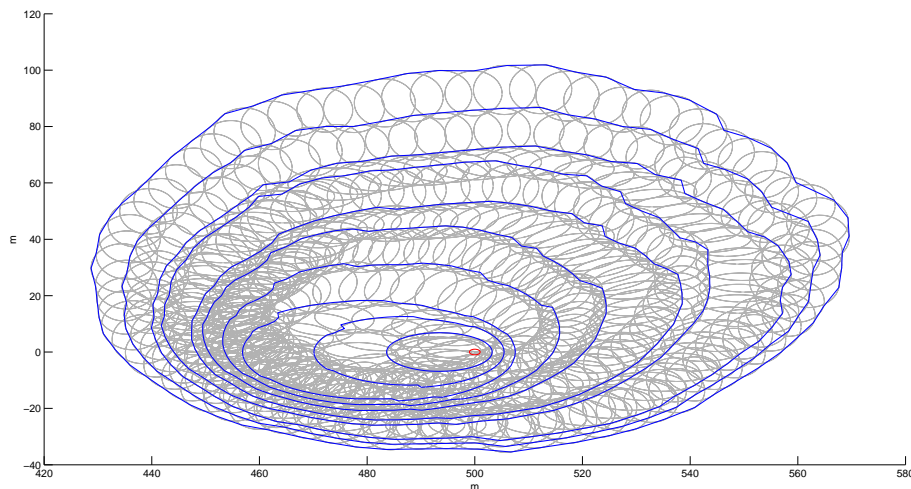


**Fig. 1.** Example of Huygens expansion with elliptical firelets (grey lines) from an ignition point (red dot in the center). Ten fire fronts with heterogeneous fuel depth and changing wind speed and direction at every time step. This Rothermel–Huygens model is also used in FARSITE (Finney, 1998).

## Forecasting wind-driven wildfires using an inverse modelling approach

O. Rios et al.

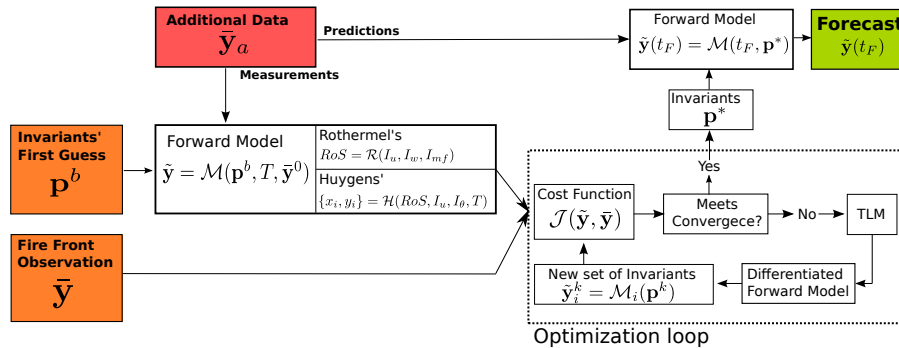


**Fig. 2.** Program structure flow diagram. Orange boxes are the required inputs, green box is the output and red box shows additional inputs.

|                          |              |
|--------------------------|--------------|
| Title Page               |              |
| Abstract                 | Introduction |
| Conclusions              | References   |
| Tables                   | Figures      |
| ◀                        | ▶            |
| ◀                        | ▶            |
| Back                     | Close        |
| Full Screen / Esc        |              |
| Printer-friendly Version |              |
| Interactive Discussion   |              |

## Forecasting wind-driven wildfires using an inverse modelling approach

O. Rios et al.

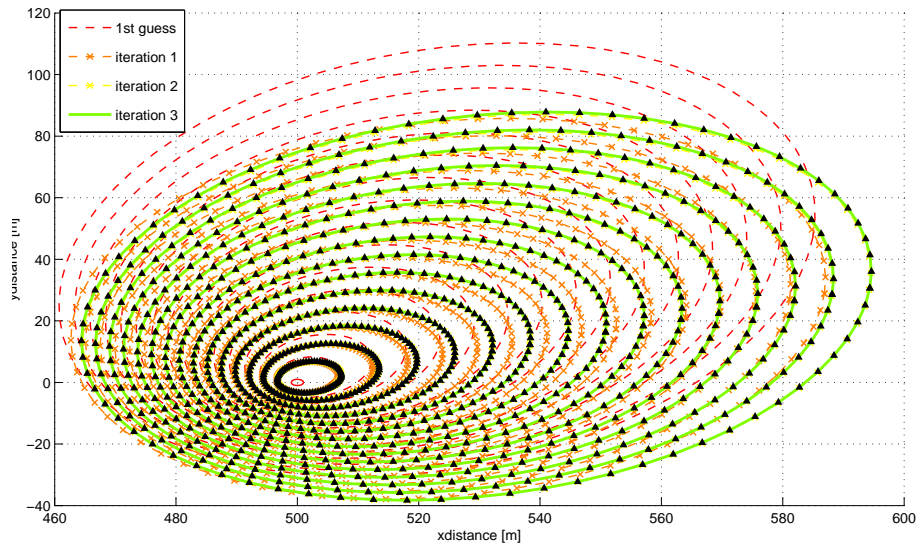


**Fig. 3.** Guess, observation, and optimisation iterations of fire fronts in an  $x$ – $y$  plane (plan view of a wildfire). The black triangles are the 15 observed positions. The red dashed lines are the fire fronts generated with the first guess and the dashed lines are the following iterations of invariants. The last iteration is depicted with green solid lines.

[Title Page](#)[Abstract](#)[Introduction](#)[Conclusions](#)[References](#)[Tables](#)[Figures](#)[⏪](#)[⏩](#)[◀](#)[▶](#)[Back](#)[Close](#)[Full Screen / Esc](#)[Printer-friendly Version](#)[Interactive Discussion](#)

Forecasting wind-driven wildfires using an inverse modelling approach

O. Rios et al.

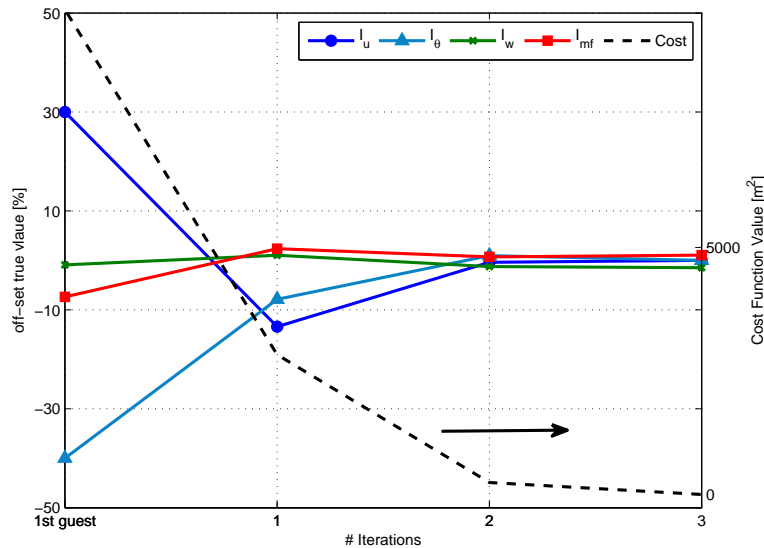


**Fig. 4.** Convergence of cost function (dashed line, right axis) and individual convergence of each invariant to the true value (solid lines, left axis) as a percentage difference. Assimilation windows = 15 min (1 assimilation  $min^{-1}$ ).

Discussion Paper | Discussion Paper | Discussion Paper | Discussion Paper | Discussion Paper

Title Page

Abstract

Introduction

Conclusions

References

Tables

Figures

◀

▶

◀

▶

Back

Close

Full Screen / Esc

Printer-friendly Version

Interactive Discussion



## Forecasting wind-driven wildfires using an inverse modelling approach

O. Rios et al.

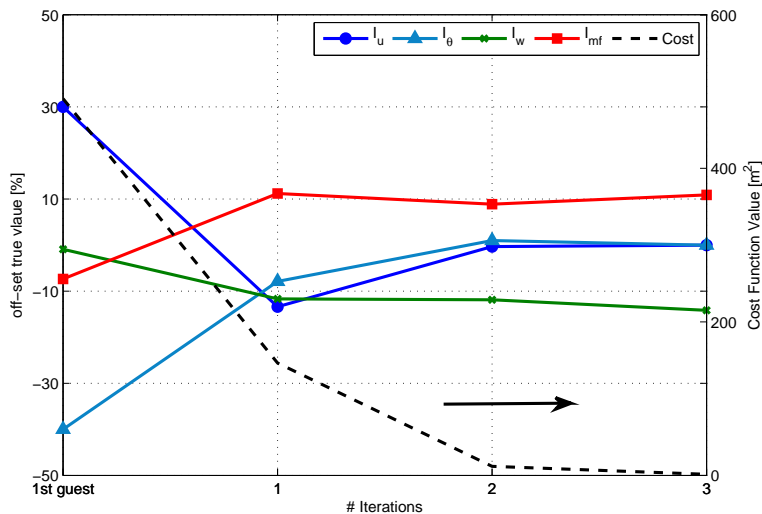


**Fig. 5.** Convergence of cost function (dashed line, right axis) and individual convergence of each invariant to true value (solid line, left axis). Assimilation windows = 3 min ( $1 \text{ assimilation min}^{-1}$ ).

**Forecasting  
wind-driven wildfires  
using an inverse  
modelling approach**

O. Rios et al.

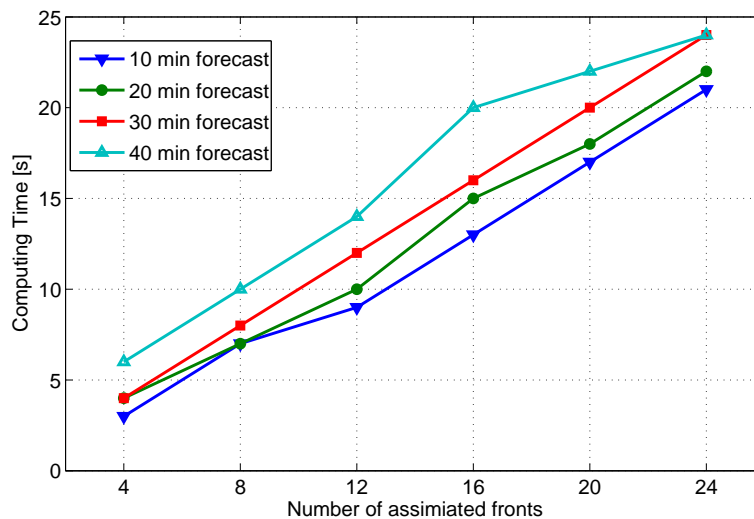


**Fig. 6.** Computing time required for 4 different forecasting windows (10, 20, 30 and 40 min) vs. the number of assimilated fire fronts.

[Title Page](#)[Abstract](#)[Introduction](#)[Conclusions](#)[References](#)[Tables](#)[Figures](#)[⏪](#)[⏩](#)[◀](#)[▶](#)[Back](#)[Close](#)[Full Screen / Esc](#)[Printer-friendly Version](#)[Interactive Discussion](#)

## Forecasting wind-driven wildfires using an inverse modelling approach

O. Rios et al.

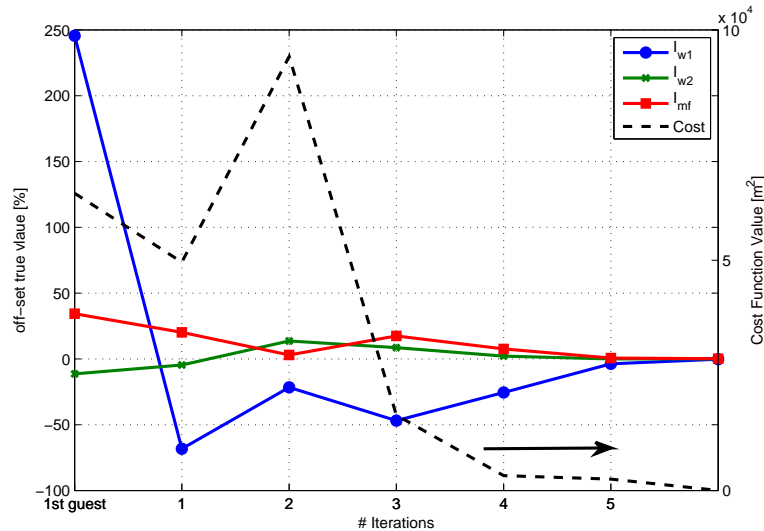


**Fig. 7.** Convergence of the cost function and the invariants when wind speed and direction are used as an input. The peak in the third iteration of the cost function is due to the correcting algorithm that resets negative values.

Title Page

Abstract

Introduction

Conclusions

References

Tables

Figures

⏪

⏩

◀

▶

Back

Close

Full Screen / Esc

Printer-friendly Version

Interactive Discussion

## Forecasting wind-driven wildfires using an inverse modelling approach

O. Rios et al.

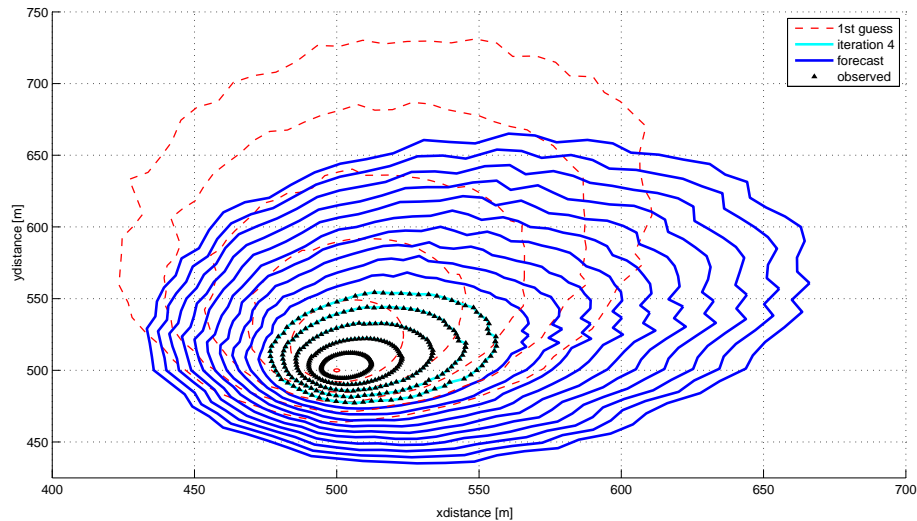


**Fig. 8.** Five assimilated fire fronts with 1 min intervals (black solid lines). The first guess (red dashed line) is taken to be far from the true invariants vector to check the algorithm capability to converge to the true invariants value. A ten min. forecast (blue solid lines) is also calculated using fuel depth as an input.

Title Page

Abstract

Introduction

Conclusions

References

Tables

Figures

◀

▶

◀

▶

Back

Close

Full Screen / Esc

Printer-friendly Version

Interactive Discussion

## Forecasting wind-driven wildfires using an inverse modelling approach

O. Rios et al.

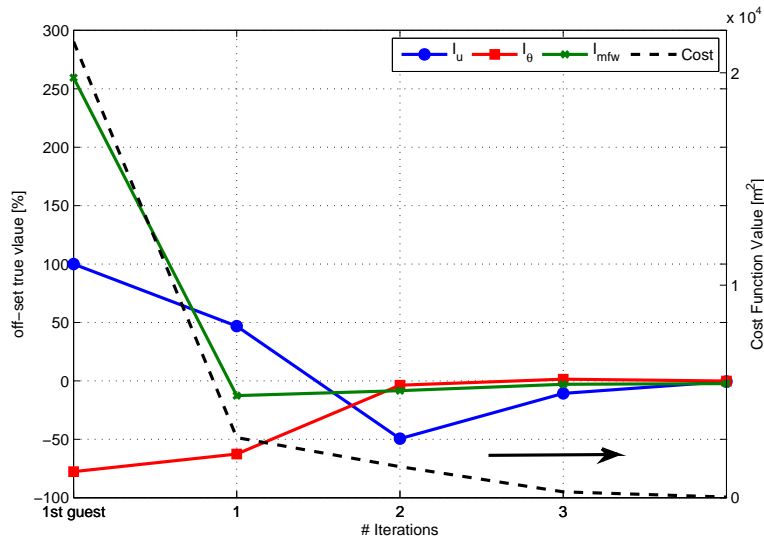


**Fig. 9.** Cost function and invariants convergence when fuel depth is input.

Title Page

|             |              |
|-------------|--------------|
| Abstract    | Introduction |
| Conclusions | References   |
| Tables      | Figures      |

⏪      ⏩  
◀      ▶  
Back      Close

Full Screen / Esc

Printer-friendly Version

Interactive Discussion



## Forecasting wind-driven wildfires using an inverse modelling approach

O. Rios et al.

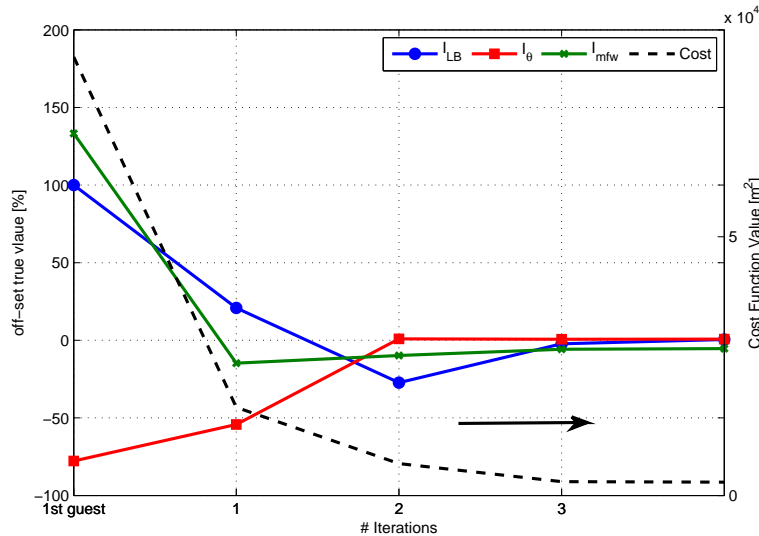


**Fig. 11.** Convergence of cost function (black dashed line) and invariants (solid lines) when perturbed data is assimilated.

Title Page

Abstract

Introduction

Conclusions

References

Tables

Figures



Back

Close

Full Screen / Esc

Printer-friendly Version

Interactive Discussion

## Forecasting wind-driven wildfires using an inverse modelling approach

O. Rios et al.

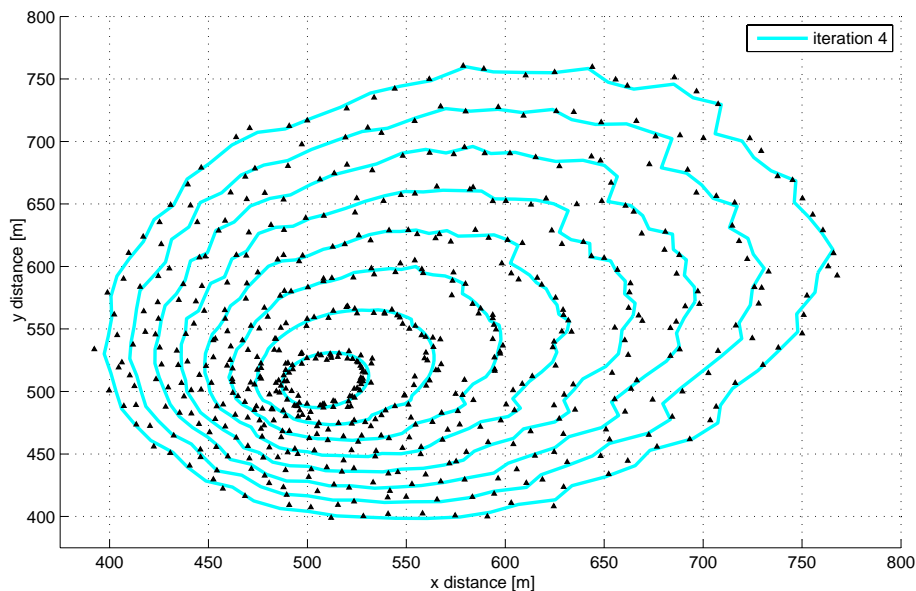


**Fig. 12.** Perturbed fire fronts (black lines) correctly assimilated after 4 integrations. The invariants cast used is this of Sect. 3.5.2 where fuel depth is used as an input and three invariants are identified.

[Title Page](#)[Abstract](#)[Introduction](#)[Conclusions](#)[References](#)[Tables](#)[Figures](#)[◀](#)[▶](#)[◀](#)[▶](#)[Back](#)[Close](#)[Full Screen / Esc](#)[Printer-friendly Version](#)[Interactive Discussion](#)